grades for non-uniformly distributed structures due to the inherent need to employ a uniform global grid. FMM or QR techniques are better suited than FFT techniques; however, neither the FMM nor the QR technique can be used at all frequencies.

This method has been developed to efficiently solve for a desired parameter of a system or device that can include both electrically large FMM elements, and electrically small QR elements. The system or device is set up as an oct-tree structure that can include regions of both the FMM type and the QR type. The system is enclosed with a cube at a 0-th level, splitting the cube at the 0-th level into eight child cubes. This forms cubes at a 1-st level, recursively repeating the splitting process for cubes at successive levels until a desired number of levels is created. For each cube that is thus formed, neighbor lists and interaction lists are maintained.

An iterative solver is then used to determine a first matrix vector product for any electrically large elements as well as a second matrix vector product for any electrically small elements that are included in the structure. These matrix vector products for the electrically large and small elements are combined, and a net delta for a combination of the matrix vector products is determined. The iteration continues until a net delta is obtained that is within the predefined limits. The matrix vector products that were last obtained are used to solve for the desired parameter. The solution for the desired parameter is then presented to a user in a tangible form; for example, on a display.

This work was done by Vikram Jandhyala and Indranil Chowdhury of the University of Washington for Johnson Space Center. For further information, contact the Johnson Technology Transfer Office at (281) 483-3809.

In accordance with Public Law 96-517, the contractor has elected to retain title to this invention. Inquiries concerning rights for its commercial use should be addressed to:

Janice C. Walsh
Federal Reporting Compliance Licensing Specialist
UW Tech Transfer
University of Washington
4322-11th Avenue, N.E., Suite 500
Seattle, WA 98105-4608
E-mail: uwinvent@u.washington.edu

Refer to MSC-24439-1, volume and number of this NASA Tech Briefs *issue, and the page number.*

Accelerated Adaptive MGS Phase Retrieval

NASA's Jet Propulsion Laboratory, Pasadena, California

The Modified Gerchberg-Saxton (MGS) algorithm is an image-based wavefront-sensing method that can turn any science instrument focal plane into a wavefront sensor. MGS characterizes optical systems by estimating the wavefront errors in the exit pupil using only intensity images of a star or other point source of light. This innovative implementation of MGS significantly accelerates the MGS phase retrieval algorithm by using stream-processing hardware on conventional graphics cards.

Stream processing is a relatively new, yet powerful, paradigm to allow parallel processing of certain applications that apply single instructions to multiple data (SIMD). These stream processors are designed specifically to support large-scale parallel computing on a single graphics chip. Computationally intensive algorithms, such as the Fast Fourier Transform (FFT), are particularly well suited for this computing environment. This high-speed version of MGS exploits commercially available hardware to accomplish the same objective in a fraction of the original time. The exploit involves performing matrix calculations in nVidia graphic cards. The graphical processor unit (GPU) is hardware that is specialized for computationally intensive, highly parallel computation.

From the software perspective, a parallel programming model is used, called CUDA, to transparently scale multicore parallelism in hardware. This technology gives computationally intensive applications access to the processing power of the nVidia GPUs through a C/C++ programming interface. The AAMGS (Accelerated Adaptive MGS) software takes advantage of these advanced technologies, to accelerate the optical phase error characterization. With a single PC that contains four nVidia GTX-280 graphic cards, the new implementation can process four images simultaneously to produce a JWST (James Webb Space Telescope) wavefront measurement 60 times faster than the previous code.

This work was done by Raymond K. Lam, Catherine M. Ohara, Joseph J. Green, Siddarayappa A. Bikkannavar, Scott A. Basinger, David C. Redding, and Fang Shi of Caltech for NASA's Jet Propulsion Laboratory. For more information, contact iaoffice@jpl.nasa.gov.

The software used in this innovation is available for commercial licensing. Please contact Daniel Broderick of the California Institute of Technology at danielb@caltech.edu. Refer to NPO-47101.

Large Eddy Simulation Study for Fluid Disintegration and Mixing

This work is directly applicable to simulations of gas turbine engines and rocket engines.

NASA's Jet Propulsion Laboratory, Pasadena, California

A new modeling approach is based on the concept of large eddy simulation (LES) within which the large scales are computed and the small scales are modeled. The new approach is expected to retain the fidelity of the physics while also being computationally efficient. Typically, only models for the small-scale fluxes of momentum, species, and enthalpy are used to reintroduce in the simulation the physics lost because the computation only resolves the large scales. These models are called subgrid (SGS) models because they operate at a scale smaller than the LES grid.

In a previous study of thermodynamically supercritical fluid disintegration and

mixing, additional small-scale terms, one in the momentum and one in the energy conservation equations, were identified as requiring modeling. These additional terms were due to the tight coupling between dynamics and real-gas thermodynamics. It was inferred that if these terms would not be modeled, the high density-gradient magnitude regions, experimentally identified as a characteristic feature of these flows, would not be accurately predicted without the additional term in the momentum equation; these high density-gradient magnitude regions were experimentally shown to redistribute turbulence in the flow. And it was also inferred that without the additional term in the energy equation, the heat flux magnitude could not be accurately predicted; the heat flux to the wall of combustion devices is a crucial quantity that determined necessary wall material properties.

The present work involves situations where only the term in the momentum equation is important. Without this additional term in the momentum equation, neither the SGS-flux constant-coefficient Smagorinsky model nor the SGS-flux constant-coefficient Gradient model could reproduce in LES the pressure field or the high density-gradient magnitude regions; the SGS-flux constant-coefficient Scale-Similarity model was the most successful in this endeavor although not totally satisfactory. With a model for the additional term in the momentum equation, the predictions of the constant-coefficient Smagorinsky and constant-coefficient Scale-Similarity models were improved to a certain extent; however, most of the improvement was obtained for the Gradient model. The previously derived model and a newly developed model for the additional term in the momentum equation were both tested, with the new model proving even more successful than the previous model at reproducing the high density-gradient magnitude regions. Several dynamic SGS-flux models, in which the SGS-flux model coefficient is computed as part of the simulation, were tested in conjunction with the new model for this additional term in the momentum equation. The most successful dynamic model was a "mixed" model combining the Smagorinsky and Gradient models.

This work is directly applicable to simulations of gas turbine engines (aeronautics) and rocket engines (astronautics).

This work was done by Josette Bellan and Ezgi Taşkinoğlu of Caltech for NASA's Jet Propulsion Laboratory. For more information, contact iaoffice@jpl.nasa.gov. NPO-47040

Tropospheric Correction for InSAR Using Interpolated ECMWF Data and GPS Zenith Total Delay

This technique could be used in environmental remote sensing applications.

NASA's Jet Propulsion Laboratory, Pasadena, California

To mitigate atmospheric errors caused by the troposphere, which is a limiting error source for spaceborne interferometric synthetic aperture radar (InSAR) imaging, a tropospheric correction method has been developed using data from the European Centre for Medium-Range Weather Forecasts (ECMWF) and the Global Positioning System (GPS).

The ECMWF data was interpolated using a Stretched Boundary Layer Model (SBLM), and ground-based GPS estimates of the tropospheric delay from the Southern California Integrated GPS Network were interpolated using modified Gaussian and inverse distance weighted interpolations. The resulting Zenith Total Delay (ZTD) correction maps have been evaluated, both separately and using a combination of the two data sets, for three short-interval InSAR pairs from Envisat during 2006 on an area stretching from northeast from the Los Angeles basin towards Death Valley. Results show that the root mean square (rms) in the InSAR images was greatly reduced, meaning a significant reduction in the atmospheric noise of up to 32 percent. However, for some of the images, the rms increased and large errors remained after applying the tropospheric correction. The residuals showed a constant gradient over the area, suggesting that a remaining orbit error from Envisat was present. The orbit reprocessing in ROI_pac and the plane fitting both require that the only remaining error in the InSAR image be the orbit error. If this is not fulfilled, the correction can be made anyway, but it will be done using all remaining errors assuming them to be orbit errors. By correcting for tropospheric noise, the biggest error source is removed, and the orbit error becomes apparent and can be corrected for.

After reprocessing the InSAR images using re-estimated satellite orbits, the overall rms reduction (using both tro-

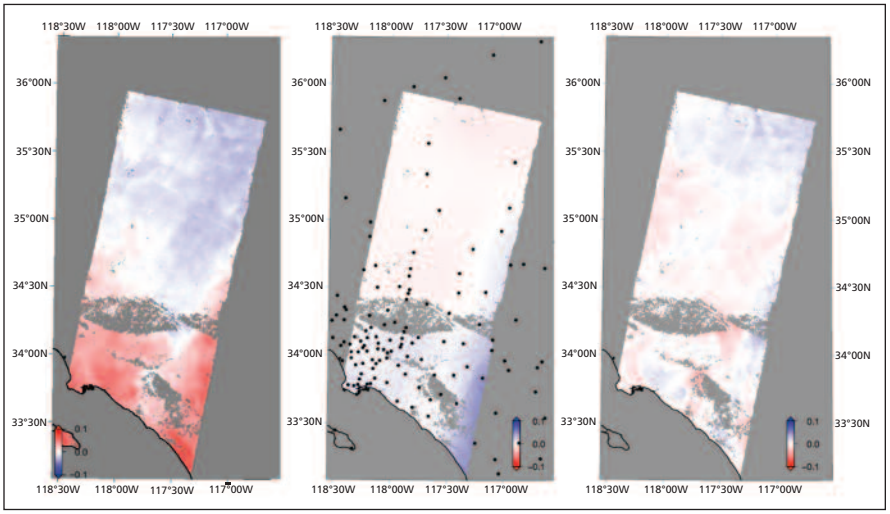

The **Original InSAR Image** (left), the **GPS ZTD Difference Correction Map** (center), and the corrected **InSAR Image** (right). The black dots in the middle image correspond to the locations of the GPS stations.